nature geoscience

ARTICLES

https://doi.org/10.1038/s41561-018-0110-z

Indian Ocean floor deformation induced by the Reunion plume rather than the Tibetan Plateau

G. Iaffaldano[1]*, D. R. Davies[2] and C. DeMets[3]

The central Indian Ocean is considered the archetypal diffuse oceanic plate boundary. Data from seismic stratigraphy and deep-sea drilling indicate that the contractional deformation of the Indian Ocean lithosphere commenced at 15.4–13.9 Ma, but experienced a sharp increase at 8–7.5 Ma. This has been maintained through to the present day, with over 80% of the shortening accrued over the past 8 Myr. Here we build on previous efforts to refine the form, timing and magnitude of the regional plate-motion changes by mitigating the noise in reconstructed Indian and Capricorn plate motions relative to Somalia. Our noise-mitigated reconstructions tightly constrain the significant speed up of the Capricorn plate over the past 8 Myr and demonstrate that the history of the Indian Ocean floor deformation cannot be explained without this plate-motion change. We propose that the Capricorn plate-motion change is driven by an increase in the eastward-directed asthenospheric flow associated with the adjacent Reunion plume, and quantitatively demonstrate the viability of this hypothesis. Our inference is supported by volcanic age distributions along the Reunion hotspot track, the anomalously high residual bathymetry of the Central Indian Ridge, full-waveform seismic tomography of the underlying asthenosphere and geochemical observations from the Central Indian Ridge. These findings challenge the commonly accepted link between the deformation of the Indian Ocean floor and the Tibetan Plateau's orogenic evolution and demonstrate that temporal variations in upwelling mantle flow can drive major tectonic events at the Earth's surface.

Plate tectonics is the paradigm that underpins the Earth sciences. It describes the motion and interaction of the lithosphere—the Earth's rigid outermost shell—and states that plates move rigidly, with the deformation concentrated at narrow plate margins. However, an ever-growing body of geophysical observations has progressively challenged such an idealization, providing evidence that some boundaries are more diffuse, with deformation extending over larger areas into the plate interiors. The central Indian Ocean is a prime example. Here the unusual abundance of intraplate earthquakes on the Indian Ocean floor[1], the widespread presence of faulted and folded sedimentary layers[2–4], and reconstructions of seafloor spreading rates at adjacent mid-ocean ridges[5–7] all indicate that what was once considered a single Indo-Australian tectonic unit is, in fact, a system of three plates—Capricorn (CP), India (IN) and Australia (AU)—separated by a wide region of diffuse deformation[8–11] (Fig. 1). This deformation is dominated by a north–south contraction[12–15], which has been linked to the Tibetan Plateau's development and to temporal variations in the convergence of the IN plate with the Eurasia (EU) plate[16], the premise being that the gravitational potential energy stored within large and growing topographic features may generate sufficient force to buckle the oceanic lithosphere[17] and resist plate convergence[18,19]. This classic and widely accepted view predicts that the timing of lithospheric deformation in the Indian Ocean be coincident with a slowdown of the IN/EU plate convergence and, accordingly, lithosphere contraction in the Indian Ocean has been linked to uplift of the Tibetan plateau[20], although a growing number of studies question such an association[21,22].

Indian Ocean lithospheric deformation and kinematics

Comprehensive analyses of seismic stratigraphy[14] and finite-rotation data sets[13,15,23] recently provided tighter constraints on the timing of the lithospheric deformation within the Indian Ocean. Seismic stratigraphy data demonstrate that the contractional deformation began at 15.4–13.9 Ma, soon after the break-up of the Indo-Australian tectonic unit[24], and that ~80% of the cumulative contraction occurred since a sharp increase in IN/CP convergence rates at 8.0–7.5 Ma, as defined by plate kinematic reconstructions[13,15]. These findings place the history of the Indian Ocean deformation in stark contrast with that of the IN/EU plate convergence since the mid-Neogene: reconstructions of the IN/EU plate convergence, for which the impact of finite-rotation data noise has been mitigated[24], demonstrate that rather than decreasing, as predicted[16], convergence increased by almost 1 cm yr^{-1} between ~11 Ma and the present day.

These findings challenge the notion that deformation of the Indian Ocean floor is a consequence of the Tibetan plateau's evolution. Here we show that it owes, instead, to the dynamics and resultant kinematics of the CP plate. Initially, we mitigate the impact of noise in kinematic reconstructions of the IN and CP plate motions relative to the Somalia (SO) plate[13,15,23]. In a result consistent with that of DeMets et al.[13], we find that the significant increase in Indian Ocean lithospheric deformation rates, at around 8 Ma, coincides with a change in the CP plate motion, as opposed to IN plate motion[13]; the implication is that the history of contractional deformation—which we infer from our noise-mitigated reconstructions and compare with that derived from a recent reassessment of the available seismic stratigraphy records[14]—cannot be explained without the CP plate-motion change. Finally, we propose that the CP plate-motion change is driven by an increase in the eastward-directed asthenospheric flow, associated with the adjacent Reunion plume, and quantitatively demonstrate the viability of this hypothesis.

We apply the REDBACK software[25,26], which mitigates the impact of finite-rotation data noise and maps the probability distribution that true plate-motion changes occurred through geological

[1]Department of Geosciences and Natural Resource Management, University of Copenhagen, Copenhagen, Denmark. [2]Research School of Earth Sciences, The Australian National University, Canberra, Australia. [3]Department of Geoscience, University of Wisconsin-Madison, Madison, WI, USA.
*e-mail: giia@ign.ku.dk

time, to high-resolution reconstructions of IN/SO and CP/SO plate motions since the Neogene[15]. Our goal is to separate true kinematic changes from the apparent changes that result directly from data noise—in doing so, REDBACK does not enforce smoothness of the finite-rotation time series and maintains the temporal resolution of the reconstructions (Methods). In our specific case, these plate-motion changes can be considered analogous to absolute plate-motion changes of the IN and CP plates, because the absolute motion of the reference plate SO did not change significantly over the Neogene[27,28].

Our analyses (Fig. 2a) indicate that a change in the IN plate motion is highly likely to have occurred before 15 Ma (driven by the break-up of the Indo-Australian plate[24]), but is less likely to have occurred since 10 Ma. Conversely, there is a high probability that the CP plate motion changed between 9 and 5 Ma and may also have changed ~15 Ma. The CP plate, rather than the IN plate, changed motion simultaneously with the sharp increase in deformation rates within the Indian Ocean lithosphere. This change amounts to an angular velocity increase of ~20% (from 0.5 to 0.61° Myr^{-1}) and an ~350 km southeastward shift of the stage Euler pole (Methods). Had deformation been caused by a sudden change in the Tibetan plateau's elevation[16,29], a marked slowdown in the kinematics of the IN and CP plates would be expected, as they are both subject to the outward gravitational push of Tibet.

The magnitude and orientation of contractional deformation of the Indian Ocean lithosphere, for which the difference between the IN and CP plate motions is a proxy, must, therefore, be linked to the CP plate-motion change. Surface velocities (Fig. 2b) and azimuths of motion (Fig. 2c), calculated at a point within the central Indian Ocean from our sets of noise-mitigated stage Euler vectors, indicate that, since ~15 Ma, the CP plate motion has been consistently faster than IN plate motion, and is also oriented in a more northerly direction. This relative motion is compatible with the observed north–south contraction of the Indian Ocean floor. The CP plate-motion change, starting at ~8 Ma (Fig. 2a), is, in fact, a speedup that is largely sustained through to the present day (Fig. 2b). We propose that this kinematic change is an accurate proxy for the sharp and significant increase in the Indian Ocean floor deformation rates. Had such a change not occurred (thin blue lines in Fig. 2b,c), the relative motion between the IN and CP plates would have been negligible, and deformation would have been smaller or accrued more slowly. This is contrary to the observations summarized above.

We use the noise-mitigated sets of stage Euler vectors for the IN and CP plates to test this notion by predicting the temporal evolution of shortening along the three profiles for which seismic stratigraphy data and dated sedimentary layers constrain the history of deformation (Fig. 3)[14]. We repeat the same calculation under the assumption that the CP plate kinematic change, identified at ~8 Ma, did not occur. When the uncertainties associated with the data are accounted for, our analyses indicate that the contraction of the oceanic lithosphere initiated at ~15 Ma, when the CP and IN plate motions became distinct in terms of both surface velocity and azimuth (Fig. 2b,c). Furthermore, the comparison of our shortening predictions with the inference from seismic stratigraphy confirms that the sudden increase of deformation rates around 8 Ma relates to the speedup in CP plate motion; removing this kinematic change from the calculation results in a clear mismatch between prediction and observation (Fig. 3). We therefore conclude that: (1) contractional deformation of the Indian Ocean lithosphere is linked to the temporal evolution of IN/CP relative motion and (2) the speedup of CP, beginning at 8 Ma and largely continuing through to the present day, is responsible for the sharp increase of deformation rates and, thus, for most (~80%) of the shortening recorded on the Indian Ocean floor. Taken together, this evidence challenges the notion that the Indian Ocean lithospheric deformation is linked to the evolution of the Tibetan plateau.

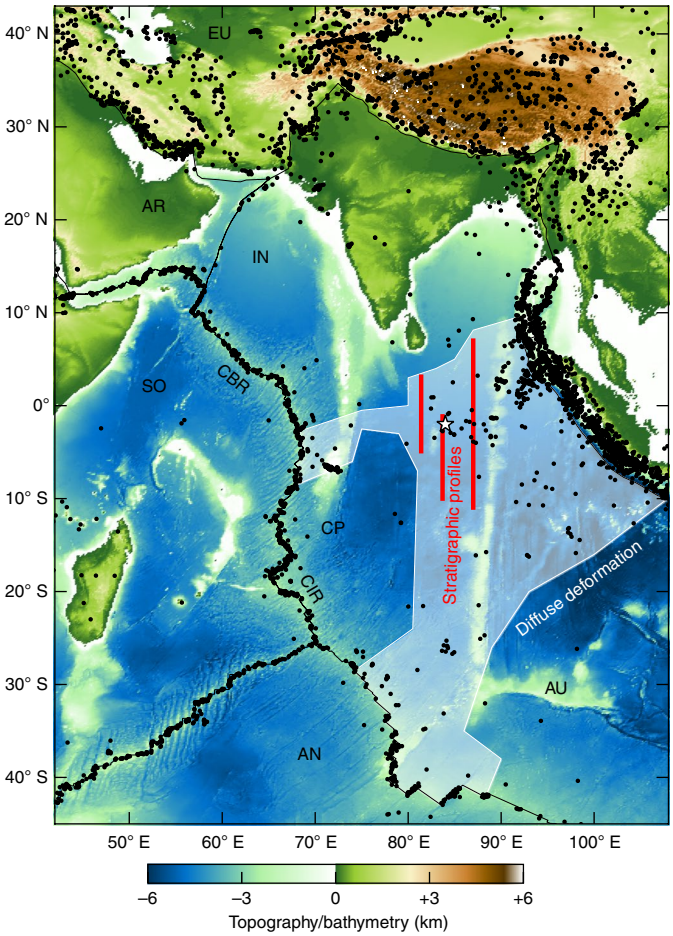

Fig. 1 | Topography/bathymetry of the central Indian Ocean region. Black dots denote the locations of earthquakes with moment magnitude $M_w > 5$, and the area of diffuse oceanic lithosphere deformation is highlighted in white. Red lines show the seismic stratigraphy profiles that constrain the Neogene history of the north–south contraction[14]. The white star indicates the location at which the surface velocities of Fig. 2 are calculated. CBR, Carlsberg Ridge; CIR, Central Indian Ridge. Tectonic plates: AN, Antarctica; AR, Arabia; AU, Australia; CP, Capricorn; EU, Eurasia; IN, India; SO, Somalia.

Reunion plume-flux impact on CP plate dynamics

We propose a driver for the speedup of CP that relates to an increase in the effective buoyancy flux of the Reunion mantle plume and the associated increase in shear stress at the base of the CP, due to Poiseuille-type asthenospheric flow[30–32]. The trace of the Reunion plume extends southwards from the Deccan traps in India (~65 Ma), along the Chagos Bank (~47 Ma), Mascarene Plateau and Nazareth Banks (~31–33 Ma), through Mauritius (~8 Ma) to the island of Reunion (present day)[33,34] (Fig. 4a). However, despite this extensive volcanic history, which spans the entire Cenozoic, there was a hiatus in volcanism from ~31 to 11 Ma, which points towards a reduction in the plume's buoyancy flux throughout this period. At ~11 Ma, however, volcanism suddenly re-emerged along the 450 km long Rodrigues Ridge, an east–west lineament that perpendicularly intersects the main hotspot track, before it progresses on to Mauritius and Reunion. The re-emergence of volcanism at this time, alongside the fact that the entire Rodrigues Ridge was built simultaneously[34], is consistent with a rapid increase in the plume's buoyancy flux at a time shortly before the CP speedup identified in our noise-mitigated reconstructions. We interpret the more-recent volcanism at Mauritius and Reunion as evidence that the increased buoyancy flux has continued through to the present day, which is consistent with a faster CP motion over the past ~8 Myr.

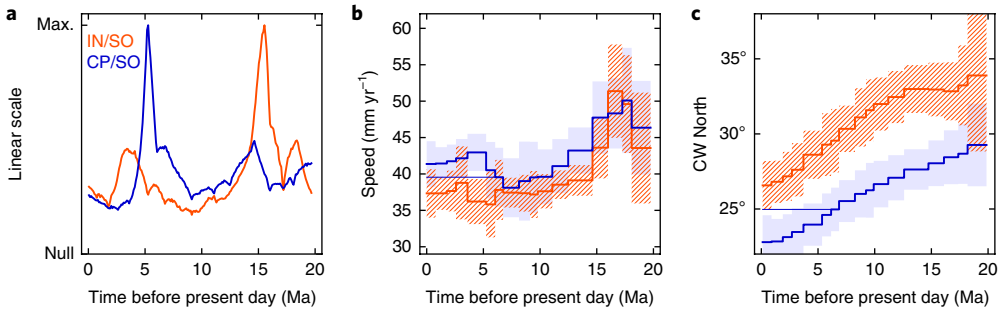

Fig. 2 | Noise-mitigated analyses of IN/SO and CP/SO Neogene plate kinematics. a, Probability distribution for a plate-motion change of the IN/SO and CP/SO kinematics. **b**,**c**, Surface velocity (**b**) and azimuth (**c**) of the motion calculated at 84.0° E, 2.0° S within the central Indian Ocean. The thin blue line shows the pattern of CP/SO motion had the kinematic change identified at ~8 Ma not occurred. The shaded areas show a 68% confidence. CW, clockwise.

If one assumes that the increased Poiseuille-type asthenospheric flow spreads radially and equally in all directions and that the plume volume is conserved (Fig. 4b), this would provide a sufficient increase in shear stress at the base of the CP to drive the plate-motion speedup identified in our analyses: specifically, the torque change associated with this process matches, within the confidence intervals, that required by the reconstructed CP-motion change (Fig. 4c,d; smaller plates, like the CP, are more susceptible to such changes (Methods)). However, there is independent evidence to suggest a more preferential eastward-flow component, towards the CP, at ~11 Ma, which further strengthens our argument. First, the Rodrigues Ridge is hypothesized to have been produced by lateral flow of Reunion plume material towards the Central Indian Ridge (CIR)[35]. Such a preferential lateral flow is probably facilitated by the thicker continental root of the Mascarene Plateau[36], which would limit plume flow towards the north and, therefore, contribute to the Rodrigues Ridge's unusual geometry. Second, our inference of a predominantly eastward flow is further supported by: (1) the unusually high present-day residual bathymetry (that is, the observed bathymetry minus that predicted by ocean-floor age through the half-space thermal model) of the CIR east of Rodrigues (Fig. 4a), where the seafloor is around 500 m shallower than that predicted by its age, with this anomalous elevation extending >1,000 km eastward; (2) recent full-waveform seismic tomography of the underlying asthenosphere[37], which images a pattern of horizontally elongated bands of low shear velocity, most prominent between 200 and 350 km depth, which extends from Reunion across the CIR and (3) geochemical analyses of samples from the CIR, which show isotopic ratios that are consistent with mixing between a mid-ocean-ridge basalt source and the Reunion plume[38].

On this basis, we repeated our torque-change calculation, but take the increased asthenospheric flow as directed eastward (Fig. 4b). Results from these analyses (Fig. 4c,d) are also able to satisfy the torque change required to generate the CP-motion change at ~8 Ma, which further establishes the viability of our hypothesis. The latter inference is compatible with the plume-flux increase estimated directly from residual bathymetry (Fig. 4d) and is viable across the range of asthenospheric viscosities and thicknesses warranted by independent observations[39,40] (Methods). The Reunion plume-flow increase systematically delivers to CP a torque of 1.8×10^{24} to 8×10^{24} N m (Fig. 4d and Supplementary Figs. 1 and 2), which is capable of driving the observed CP speedup. The associated force per unit length, rigidly transmitted by the CP to the ~2,000 km wide deformation area of the Indian Ocean, is, thus, in the range 1.4×10^{11} to 6×10^{11} N m^{-1}. Such a force is sufficient to buckle the upper layer of the oceanic lithosphere under horizontal compression (Methods) and, therefore, to generate the observed contractional deformation of the Indian Ocean floor. We therefore propose that the CP speedup at 8 Ma and contemporaneous deformation across the Indian Ocean floor are a consequence of an increase in the buoyancy flux of the Reunion mantle plume prior to the formation of the Rodrigues Ridge, and an increase in the flow of Reunion plume material, towards the CIR, after its emergence south of the Mascarene plateau. Our results demonstrate the need to decouple the evolution of the Tibetan Plateau from Indian Ocean deformation and further highlight the important role played by upwelling mantle flow[41,42] and asthenospheric dynamics[30–32,43–45] in shaping surface tectonics.

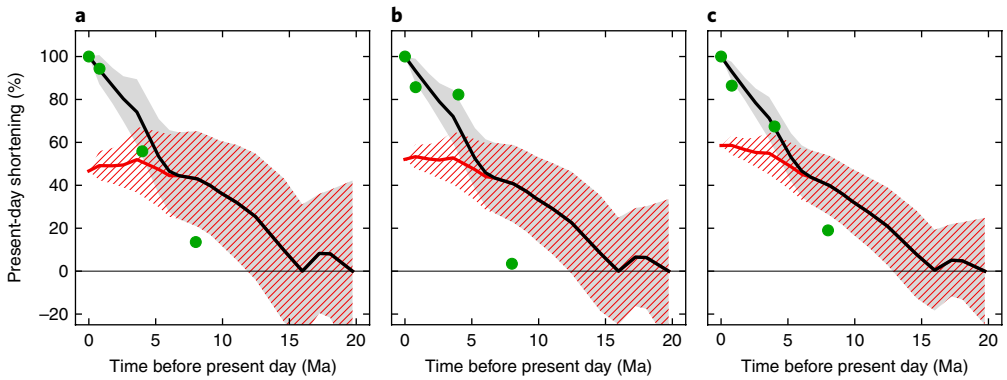

Fig. 3 | History of shortening within the central Indian Ocean. a, Shortening along the profile at longitude 81.4° E (Fig. 1) inferred from seismic stratigraphy (green circles)[14] and predicted by the noise-mitigated IN/CP motion (black). Red shows the latter, but assuming no kinematic change at ~8 Ma (that is, corresponding to the thin blue line of Fig. 2). Grey shaded and red hatched areas indicate the 68% confidence intervals. **b**,**c**, As in **a**, but for profiles along longitudes 83.7° E (**b**) and 87.0° E (**c**), respectively.

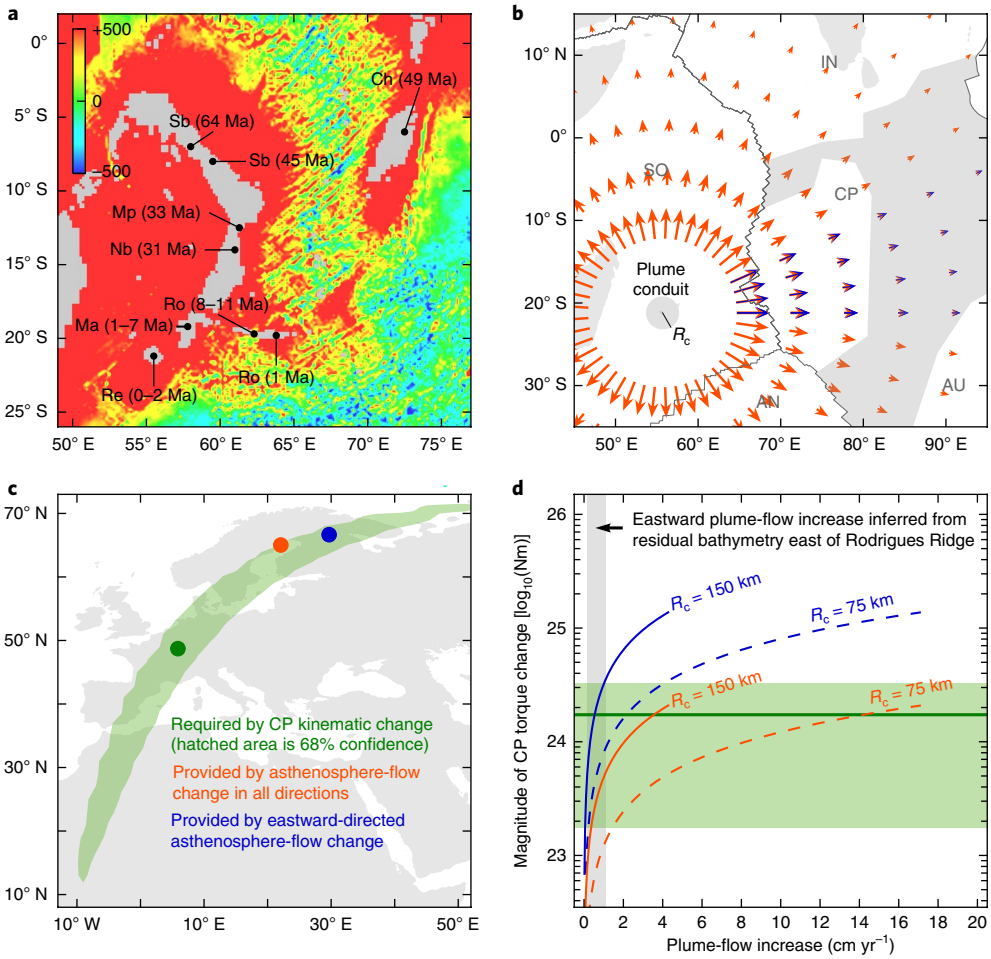

Fig. 4 | Mechanism that drives the 8 Ma CP-motion change. a, Residual bathymetry (m) and ages of volcanic rock samples (grey areas are shallower than −2 km). Re, Reunion; Ro, Rodrigues; Ma, Mauritius; Nb, Nazareth Bank; Mp, Mascarene plateau; Sb, Saya de Malha Bank; Ch, Chagos. **b**, Patterns of increased asthenosphere flow induced by an increase in the Reunion plume flux (R_C is plume-conduit radius shown by the stippled circle). The orange arrows show the flow change that spreads to the asthenosphere radially and equally in all directions, whereas the blue arrows show the preferential eastward-directed flow change. **c**, Poles of the CP torque-change vector. **d**, Magnitude of the CP torque-change vector ($\mu_A = 6\times10^{19}$ Pa s, $H_A = 110$ km, $\mu_{UM} = 4\times10^{21}$ Pa s (Methods)) for different values of the plume-conduit radius (the largest values are limited by the Reunion plume's present-day buoyancy flux[53]). The values of the Reunion plume-flow increase that matches the required torque change (that is, where blue and orange profiles intersect the green area) correspond to ~25 to ~35% of the present-day Reunion buoyancy flux. Key as in **c**.

Methods

Methods, including statements of data availability and any associated accession codes and references, are available at https://doi.org/10.1038/s41561-018-0110-z.

Received: 31 October 2017; Accepted: 21 March 2018;
Published online: 23 April 2018

References

1. Stein, S. & Okal, E. A. Seismicity and tectonics of the Ninetyeast Ridge area: evidence for internal deformation of the Indian plate. *J. Geophys. Res.* **83**, 2233–2245 (1978).
2. Bull, J. M. & Scrutton, R. A. Seismic reflection images of intraplate deformation, central Indian Ocean, and their tectonic significance. *J. Geol. Soc. Lond.* **149**, 955–966 (1992).
3. Krishna, K. S. et al. Periodic deformation of oceanic crust in the central Indian Ocean. *J. Geophys. Res.* **103**, 17859–17875 (1998).
4. Curray, J. R., Emmel, F. J. & Moore, D. G. The Bengal Fan: morphology, geometry, stratigraphy, history and processes. *Mar. Pet. Geol.* **19**, 1191–1223 (2002).
5. Wiens, D. A. et al. A diffuse plate boundary model for Indian Ocean tectonics. *Geophys. Res. Lett.* **12**, 429–432 (1985).
6. Gordon, R. G., Stein, S., DeMets, C. & Argus, D. F. Statistical tests for closure of plate motion circuits. *Geophys. Res. Lett.* **14**, 587–590 (1987).
7. Royer, J. Y. & Chang, T. Evidence for relative motions between the Indian and Australian plates during the last 20 m.y. from plate tectonic reconstructions: implications for the deformation of the Indo–Australian plate. *J. Geophys. Res.* **96**, 11779–11802 (1991).
8. DeMets, C., Gordon, R. G. & Vogt, P. Location of the Africa–Australia–India triple junction and motion between the Australian and Indian plates: results from an aeromagnetic investigation of the Central Indian and Carlsberg ridges. *Geophys. J. Int.* **119**, 893–930 (1994).
9. Royer, J. Y. & Gordon, R. G. The motion and boundary between the Capricorn and Australian plates. *Science* **277**, 1268–1274 (1997).
10. Gordon, R. G. The plate tectonic approximation: plate nonrigidity, diffuse plate boundaries, and global plate reconstructions. *Annu. Rev. Earth Planet. Sci.* **26**, 615–642 (1998).
11. Zatman, S., Gordon, R. G. & Richards, M. A. Analytic models for the dynamics of diffuse oceanic plate boundaries. *Geophys. J. Int.* **145**, 145–156 (2001).
12. Gordon, R. G., DeMets, C. & Royer, J. Y. Evidence for long-term diffuse deformation of the lithosphere of the equatorial Indian Ocean. *Nature* **395**, 370–374 (1998).
13. DeMets, C., Gordon, R. G. & Royer, J.-Y. Motion between the Indian, Capricorn and Somalian plates since 20 Ma: implications for the timing and magnitude of distributed lithospheric deformation in the equatorial Indian Ocean. *Geophys. J. Int.* **161**, 445–468 (2005).
14. Krishna, K. S., Bull, J. M. & Scrutton, R. A. Early (pre-8 Ma) fault activity and temporal strain accumulation in the central Indian Ocean. *Geology* **37**, 227–230 (2009).

15. Bull, J. M., DeMets, C., Krishna, K. S., Sanderson, D. J. & Merkouriev, S. Reconciling plate kinematic and seismic estimates of lithospheric convergence in the central Indian Ocean. *Geology* **38**, 307–310 (2010).
16. Molnar, P., England, P. & Martinod, J. Mantle dynamics, uplift of the Tibetan plateau, and the Indian monsoon. *Rev. Geophys.* **31**, 357–396 (1993).
17. Weissel, J. K., Anderson, R. N. & Geller, C. A. Deformation of the Indo–Australian plate. *Nature* **287**, 284–291 (1980).
18. Iaffaldano, G., Bunge, H.-P. & Dixon, T. H. Feedback between mountain belt growth and plate convergence. *Geology* **34**, 893–896 (2006).
19. Copley, A., Avouac, J.-P. & Royer, J.-Y. India–Asia collision and the Cenozoic slowdown of the Indian plate: implications for the forces driving plate motions. *J. Geophys. Res.* **115**, B03410 (2010).
20. Molnar, P. & Stock, J. M. Slowing of India's convergence with Eurasia since 20 Ma and its implications for Tibetan mantle dynamics. *Tectonics* **28**, TC3001 (2009).
21. Rowley, D. B. & Currie, B. S. Palaeo-altimetry of the late Eocene to Miocene Lunpola basin, central Tibet. *Nature* **439**, 677–681 (2006).
22. Priestley, K., Jackson, J. & McKenzie, D. Lithospheric structure and deep earthquakes beneath India, the Himalaya and southern Tibet. *Geophys. J. Int.* **172**, 345–362 (2008).
23. Merkouriev, S. & DeMets, C. Constraints on Indian plate motion since 20 Ma from dense Russian magnetic data: implications for Indian plate dynamics. *Geochem. Geophys. Geosystems* **7**, Q02002 (2006).
24. Iaffaldano, G., Bodin, T. & Sambridge, M. Slow-downs and speed-ups of India–Eurasia convergence since ~20 Ma: data-noise, uncertainties and dynamic implications. *Earth Planet. Sci. Lett.* **367**, 146–156 (2013).
25. Iaffaldano, G., Bodin, T. & Sambridge, M. Reconstructing plate-motion changes in the presence of finite-rotations noise. *Nat. Commun.* **3**, 1048 (2012).
26. Iaffaldano, G., Hawkins, R., Bodin, T. & Sambridge, M. REDBACK: open-source software for efficient noise-reduction in plate kinematic reconstructions. *Geochem. Geophys. Geosystems* **15**, 1663–1670 (2014).
27. Torsvik, T. H., Steinberger, B., Gurnis, M. & Gaina, C. Plate tectonics and net lithosphere rotation over the past 150 My. *Earth Planet. Sci. Lett.* **291**, 106–112 (2010).
28. Iaffaldano, G. & DeMets, C. Late Neogene changes in North America and Antarctica absolute plate motions inferred from the Mid-Atlantic and Southwest Indian Ridges spreading histories. *Geophys. Res. Lett.* **43**, 8466–8472 (2016).
29. Harrison, T. M., Copenald, P., Kidd, W. S. F. & Yin, A. Raising Tibet. *Science* **255**, 1663–1670 (1992).
30. Hoeink, T. & Lenardic, A. Three-dimensional mantle convection simulations with a low-viscosity asthenosphere and the relationship between heat flow and the horizontal length scale of convection. *Geophys. Res. Lett.* **35**, L10304 (2008).
31. Hoeink, T. & Lenardic, A. Long wavelength convection, Poiseuille–Couette flow in the low-viscosity asthenosphere and the strength of plate margins. *Geophys. J. Int.* **180**, 23–33 (2010).
32. Natarov, S. I. & Conrad, C. P. The role of Poiseuille flow in creating depth-variation of asthenospheric shear. *Geophys. J. Int.* **190**, 1297–1310 (2012).
33. Duncan, R. & Richards, M. Hotspots, mantle plumes, flood basalts, and true polar wander. *Rev. Geophys.* **29**, 31–50 (1991).
34. Duncan, R. & Storey, M. in *The Life Cycle of Indian Ocean Hotspots*, Vol. 29 (eds Duncan, R. A. et al.) 91–103 (American Geophysical Union, Washington, DC, 1992).
35. Morgan, W. J. Rodriguez, Darwin, Amsterdam, …, a second type of hotspot island. *J. Geophys. Res.* **83**, 5355–5360 (1978).
36. Torsvik, T. H. et al. A Precambrian microcontinent in the Indian Ocean. *Nat. Geosci.* **6**, 223–227 (2013).
37. French, S., Lekic, V. & Romanowicz, B. Waveform tomography reveals channeled flow at the base of the oceanic asthenosphere. *Science* **342**, 227–230 (2013).
38. Murton, B. M., Tindle, A. E., Milton, J. A. & Sauter, D. Heterogeneity in southern central Indian ridge MORB: implications for ridge–hot spot interaction. *Geochem. Geophys. Geosystems* **6**, Q03E20 (2005).
39. Paulson, A. & Richards, M. A. On the resolution of radial viscosity structure in modelling long-wavelength postglacial rebound data. *Geophys. J. Int.* **179**, 1516–1526 (2009).
40. Iaffaldano, G. & Lambeck, K. Pacific plate-motion change at the time of the Hawaiian–Emperor bend constrains the viscosity of Earth's asthenosphere. *Geophys. Res. Lett.* **41**, 3398–3406 (2014).
41. Cande, S. C. & Stegman, D. R. Indian and African plate motions driven by the push force of the Reunion plume head. *Nature* **475**, 47–52 (2011).
42. van Hinsbergen, D. J. J., Steinberger, B., Doubrovine, P. V. & Gassmöller, R. Acceleration and deceleration of India–Asia convergence since the Cretaceous: roles of mantle plumes and continental collision. *J. Geophys. Res.* **116**, B06101 (2011).
43. Ballmer, M. D., Conrad, C. P., Smith, E. I. & Harmon, N. Non-hotspot volcano chains produced by migration of shear-driven upwelling toward the East Pacific Rise. *Geology* **41**, 479–482 (2013).
44. Hawley, W. B., Allen, R. M. & Richards, M. A. Tomography reveals buoyant asthenosphere accumulating beneath the Juan de Fuca plate. *Science* **353**, 1406–1408 (2016).
45. Stotz, I. L., Iaffaldano, G. & Davies, D. R. Pressure-driven Poiseuille flow: a major component of the torque-balance governing Pacific plate motion. *Geophys. Res. Lett.* **45**, 117–125(2018).
53. Sleep, N. H. Hotspots and mantle plumes: some phenomenology. *J. Geophys. Res.* **95**, 6715–6736 (1990).

Acknowledgements

G.I. acknowledges support from the Department of Geosciences and Natural Resource Management at the University of Copenhagen. D.R.D. acknowledges support from the Australian Research Council, under grant nos FT140101262 and DP170100058. The authors are grateful to R. Gordon and A. Whitchurch for constructive comments that improved this study.

Author contributions

G.I. conceived the study. G.I. and C.D. undertook the noise-mitigation analysis. G.I. performed the calculations of lithosphere shortening, residual bathymetry and torque changes. D.R.D. undertook the analysis of volcanism along the Reunion hotspot track and tied in associated interdisciplinary observational constraints. All the authors contributed to discussing and writing the paper.

Competing interests

The authors declare no competing interests.

Additional information

Supplementary information is available for this paper at https://doi.org/10.1038/s41561-018-0110-z.

Reprints and permissions information is available at www.nature.com/reprints.

Correspondence and requests for materials should be addressed to G.I.

Publisher's note: Springer Nature remains neutral with regard to jurisdictional claims in published maps and institutional affiliations.

Methods

Noise mitigation using REDBACK software. REDBACK is open-source software that implements trans-dimensional hierarchical Bayesian inference[46,47] to mitigate the impact of finite-rotation noise on stage Euler vectors, and thus on reconstructed plate motions[25,26]. To achieve this, REDBACK generates millions of models of a time series of finite rotations, and compares these to the noisy reconstruction at hand. On the basis of the discrepancy between model and reconstruction, REDBACK accepts or rejects a particular model—the threshold for acceptance is randomly selected for every model to avoid local discrepancy minima within the model space. REDBACK assigns to each accepted model a probability of being a faithful realization of the truth on the basis of the discrepancy from the noisy reconstruction. Next, REDBACK modifies the previously accepted model to generate a new one to compare to the data. Such a modification is randomly selected among five possibilities: (1) modify the magnitude of an existing plate-motion change within the previously accepted model, (2) modify the time of an existing plate-motion change within the previously accepted model, (3) remove an existing plate-motion change from the previously accepted model, (4) add a new plate-motion change to the previously accepted model and (5) rescale either upwards or downwards the nominal covariances of the reconstruction. The intrinsic temporal resolution of the models (that is, the number of finite rotations that span the interval of time covered by the noisy reconstruction) is typically >10 times finer than the reconstruction resolution. These features avoid the loss of temporal resolution and enforce smoothness between specific points in time, among others. The output time series of finite rotations and stage Euler vectors are calculated as the weighted average of all the accepted models. More details on REDBACK are given in previous studies[25,26].

Noise mitigation on CP/SO and IN/SO plate motions. We used REDBACK to mitigate the impact of finite-rotation noise in reconstructions of CP/SO and IN/SO plate motions since around 20 Ma (ref. [15]). REDBACK parameters are listed in Supplementary Tables 1 and 2. Finite rotations and stage Euler vectors, following noise mitigation, are listed in Supplementary Tables 3 and 4.

Lithospheric shortening within the central Indian Ocean. Observed shortening is the strain inferred from seismic stratigraphy and deep-sea drilling multiplied by the length of the seismic profiles[14]. To calculate the predicted shortening, we first reconstruct the past positions of the North and South ends of the seismic profiles using the noise-mitigated kinematics of the IN plate (for the North end) and the CP plate (for the South end) relative to SO. Next, we calculated the geodesic distance between the reconstructed past positions through geological time. We calculated the 68% confidence intervals using one-million samples of finite rotations drawn from the noise-mitigated series.

Residual bathymetry and inferred plume-flow increase. We calculated the residual bathymetry by subtracting from the observed bathymetry[48], a prediction based upon the age of the ocean floor[49] using a published model[50]. We find that the residual bathymetry to the east of Rodrigues is in the range 300–500 m and extends for 1,000–2,500 km. We calculated the associated Reunion plume-flow increase by requiring that it be equal to the asthenospheric Poiseuille-type flow (Δv_{PF}) induced by a pressure (Δp) gradient that arises from the bathymetry residual. The relevant equation is:

$$\Delta v_{PF} = \frac{H_A^2}{8\mu_A}\frac{\Delta p}{\Delta l} = \frac{H_A^2}{8\mu_A}\frac{\Delta h \times g \times \Delta\rho_{LW}}{\Delta l} \quad (1)$$

where μ_A and H_A are the viscosity and thickness of the asthenosphere, g is the gravitational acceleration on the Earth's surface (9.8 m s^{-2}), $\Delta\rho_{LW}$ is the density contrast between the oceanic crust and seawater (~1,800 kg m^{-3}), Δh is the residual bathymetry (in the range 300–500 m) and Δl is its lateral extent (in the range 1,000–2,500 km).

Torque changes. To calculate the torque change $\Delta\mathbf{M}_{CP}$ required to explain the change in CP motion starting at 8 Ma ($\Delta\boldsymbol{\omega}_{CP}$), along with the 68% confidence range, we build on previous studies that derived equations to calculate torques upon tectonic plates[51,52] independent of any assumptions on driving mechanisms[52]. We use the formula[52]:

$$\Delta\mathbf{M}_{CP} = \int_{A_{CP}} \mathbf{r} \times \frac{2\mu_A}{H_A}(\Delta\boldsymbol{\omega}_{CP} \times \mathbf{r})\,\mathrm{d}A_{CP}(\mathbf{r}) \quad (2)$$

where $\mathbf{r}$ is the position vector of the generic point on the lithosphere base of CP and A_{CP} is the spherical area of the lithosphere base of CP, which in our calculation varies laterally depending on the ocean-floor age[49] at $\mathbf{r}$. We drew one-million samples of $\Delta\boldsymbol{\omega}_{CP}$ using the eighth (6.733–8.132 Ma) and fifth (3.596–5.235 Ma) stages of the CP Euler vector series in Supplementary Table 5. From these, we obtained one-million samples of $\Delta\mathbf{M}_{CP}$. We calculated the 68% confidence interval on the magnitude of the torque change required as the interval in which 68% of the samples of $|\Delta\mathbf{M}_{CP}|$ occur. Similarly, we calculated the 68% confidence region around the pole of the torque change required as the geographical region in which 68% of the samples of $\Delta\mathbf{M}_{CP}/|\Delta\mathbf{M}_{CP}|$ occur.

We calculated the torque change ($\Delta\mathbf{M}_{PF}$) provided by a generic Reunion plume-flow increase ($\Delta\mathbf{v}_{PF}$) using the formula[52]:

$$\Delta\mathbf{M}_{PF} = \int_{A_{CP}} \mathbf{r} \times \frac{2\mu_A}{H_A}\Delta\mathbf{v}_{PF}(\mathbf{r})\,\mathrm{d}A_{CP}(\mathbf{r}) \quad (3)$$

where the direction of $\Delta\mathbf{v}_{PF}(\mathbf{r})$ is determined by the specific pattern used (Fig. 4b and Supplementary Fig. 2a). The magnitude $|\Delta\mathbf{v}_{PF}|$ (that is, the plume flow) is kept as a free parameter that we took in the range from zero to what is dictated by the present-day Reunion buoyancy flux[53], assuming a density contrast of 30 kg m^{-3} between the plume and background mantle and assuming the plume-conduit radius (75 or 150 km). We use values for the ratio μ_A/H_A constrained jointly from glacial rebound data and modelling of the plate dynamics (further details are given elsewhere[39,40,45]).

Buckling of a plate under a horizontal force. The theory of elasticity and flexure predicts that a thin plate subject to a horizontal compressive force per unit length will buckle if such a force exceeds the minimum value:

$$F_m = \frac{\pi^2}{L^2}\frac{EH_e^3}{12(1-\nu^2)} \quad (4)$$

where L is the extent of the deforming layer along the direction of F, E and ν are, respectively, Young's modulus and Poison's ratio, and H_e is the equivalent elastic thickness of the deforming layer[54]. The deforming part of the Indian Ocean lithosphere (L in the range 2,000–2,500 km) features an age between ~40 and ~80 Ma. This means that the equivalent elastic thickness (H_e) of the upper, deforming layer of the oceanic lithosphere is, at most, in the range 5–25 km (ref. [55]). Furthermore, the upper part of the oceanic lithosphere features E in the range 0.06–0.1 TPa and ν in the range 0.15–0.3 (ref. [54]). We map the probability density distribution (PDD) of F_m from an ensemble of 10^8 samples of L, E, ν and H_e uniformly distributed within the ranges above. Supplementary Fig. 3 compares the the PDD of F_m with the range of force delivered by the Reunion plume-flux increase. The latter one is larger than the most-probable value of F_m (~2×10^9 N m^{-1}), and, in the most stringent conditions, larger than 90% of the PDD.

Code availability. REDBACK is released open source under the GNU General Public License and can be obtained at http://www.iearth.org.au/codes/REDBACK.

Data availability. The authors declare that the data supporting the findings of this study are available within the article and its Supplementary Information files.

References

46. Malinverno, A. & Briggs, V. A. Expanded uncertainty quantification in inverse problems: hierarchical Bayes and empirical Bayes. *Geophysics* **69**, 1005–1016 (2004).
47. Sambridge, M., Gallagher, K., Jackson, A. & Rickwood, P. Trans-dimensional inverse problems, model comparison and the evidence. *Geophys. J. Int.* **167**, 528–542 (2006).
48. Smith, W. H. F. & Sandwell, D. T. Global sea floor topography from satellite altimetry and ship depth soundings. *Science* **277**, 1956–1962 (1997).
49. Gibbons, A. D., Zahirovic, S., Muller, R. D., Whittaker, J. M. & Yatheesh, V. A tectonic model reconciling evidence for the collisions between India, Eurasia and intra-oceanic arcs of the central–eastern Tethys. *Gondwana Res.* **28**, 451–492 (2015).
50. Stein, C. A. & Stein, S. A model for the global variation in oceanic depth and heat flow with lithospheric age. *Nature* **359**, 123–129 (1992).
51. Chapple, W. M. & Tullis, T. E. Evaluation of the forces that drive the plates. *J. Geophys. Res.* **82**, 1967–1984 (1977).
52. Iaffaldano, G. & Bunge, H.-P. Rapid plate motion variations: observations serving geodynamic interpretation. *Annu. Rev. Earth Planet. Sci.* **43**, 571–592 (2015).
54. Turcotte, D. & Schubert, G. *Geodynamics* (Cambridge Univ. Press, Cambridge, 2002).
55. Watts, A. B. *Isostasy and Flexure of the Lithosphere* (Cambridge Univ. Press, Cambridge, 2001).